XLVI CILAMCE
VITÓRIA - ES - BRAZIL - 2025
XLVI IBERO-LATIN AMERICAN CONGRESS ON COMPUTATIONAL METHODS IN ENGINEERING

Dynamic Catenary: Efficient Modeling of Heterogeneous Mooring Lines

Milton M. G. dos Santos[1], Eduardo N. Lages[2]

Laboratório de Computação Científica e Visualização, Universidade Federal de Alagoas
Av. Lourival Melo Mota s/n, Cidade Universitária, CEP: 57072-970, Maceió/AL, Brasil
[1]*milton.santos@ctec.ufal.br*, [2]*enl@lccv.ufal.br*

Abstract. This study presents Dynamic Catenary (DynCat), an extended methodology for simulating elastic mooring lines in free-catenary configurations connected to floating offshore units. Traditional analyses rely either on catenary models, which are computationally efficient but dynamically oversimplified, or on finite element models (FEM), which provide higher fidelity at a greater computational cost. DynCat bridges this gap by combining the low computational cost of catenary models with enhanced physical accuracy, grounded in principles of deformable-solid mechanics. The formulation revisits deformable cable elements within the FEM framework, assembles multi-material line segments into a unified model, and incorporates environmental loading effects, resulting in numerically stable simulations that provide instantaneous line geometry and tension profiles at each time step. Validation studies covering shallow, intermediate, and deep waters under various fairlead motion regimes demonstrate that DynCat maintains good accuracy under low-to-moderate motion conditions. Although its performance deteriorates under highly dynamic deep-water conditions, DynCat remains accurate and robust within the operational envelope of shallow-to-intermediate water depths and low-to-moderate motion intensities, with simulation time reductions of 60–70% compared to conventional FEM approaches. This makes DynCat a promising tool for preliminary design and time-constrained analyses.

Keywords: Mooring lines, Cable structures, Morison's forces, Numerical simulation, Computational efficiency.

1 Introduction

Offshore oil exploration poses considerable technical challenges to the structural design and operation of floating units. Mooring lines are critical structural elements for the stability and station-keeping of floating units, transmitting restoring forces that limit undesired displacements induced by environmental loads. To address the nonlinear behavior of mooring lines — governed by installation geometry, material properties, and the magnitude of dynamic loads — two distinct modeling approaches can be adopted: catenary models, which are computationally efficient but less accurate representations of the physical problem; and numerical models based on the Finite Element Method (FEM), such as those implemented in the DOOLINES framework [1], which provide higher accuracy at the expense of greater computational cost. Numerous efforts have been made to combine physical representativeness with low computational cost, leading to the development of models that employ time integration algorithms — such as the Local Discontinuous Galerkin (LDG-FEM) [2] and Lumped Mass (LM-FEM) [3] formulations for dynamic analyses, and the Piecewise Extrapolation Method (PEM) [4,5] for quasi-static (QS) simulations — as well as QS models that avoid time integration, such as the Quasi-Dynamic model [6]. In this context, a QS model free for time integration algorithms is proposed — offering a more realistic dynamic representation than classical catenaries while being less computationally demanding than FEM. The Dynamic Catenary (DynCat) method is a hybrid approach that combines the analytical simplicity of the classical catenary with a stable dynamic representation, incorporating the primary inertial and drag effects in a homogenized manner. The proposed methodology is structured in the following stages: a) Cable structures under general loadings formulation; b) Kinematic analysis of the line; c) Modeling of dynamic actions and their incorporation into the structural model, ensuring numerical stability, and; d) Reconstruction of the line, enabling its dynamic simulation.

2 Methodology

The proposed methodology models the mooring line as a system of elastic cables in a catenary configuration, subdivided into segments with distinct physical properties. The adopted formulation builds upon the cable structures under general loadings theory, developed by Abad et al. [7], enabling the consideration of segments with distinct axial stiffnesses, linear mass densities, and hydrodynamic coefficients. The simulation advances incrementally in time, starting from kinematic estimates derived from a sequence of deformable static states, updated according to the fairlead motion, enabling the computation and incorporation of dynamic actions into the structural model. The flowchart presented in Fig. 1 describes the incremental process over time.

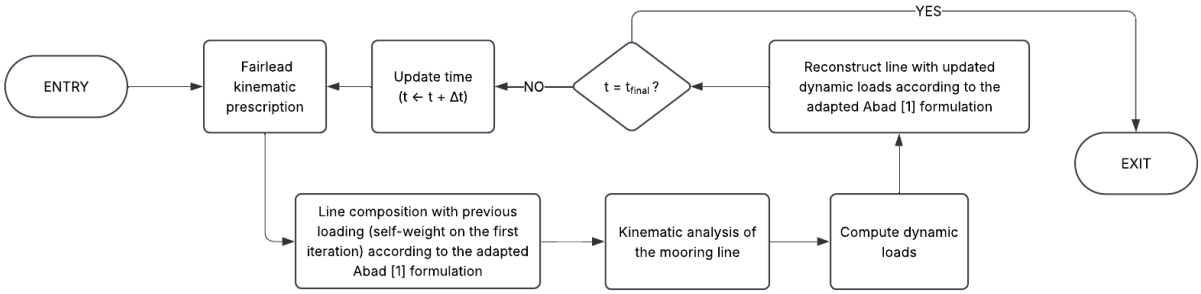
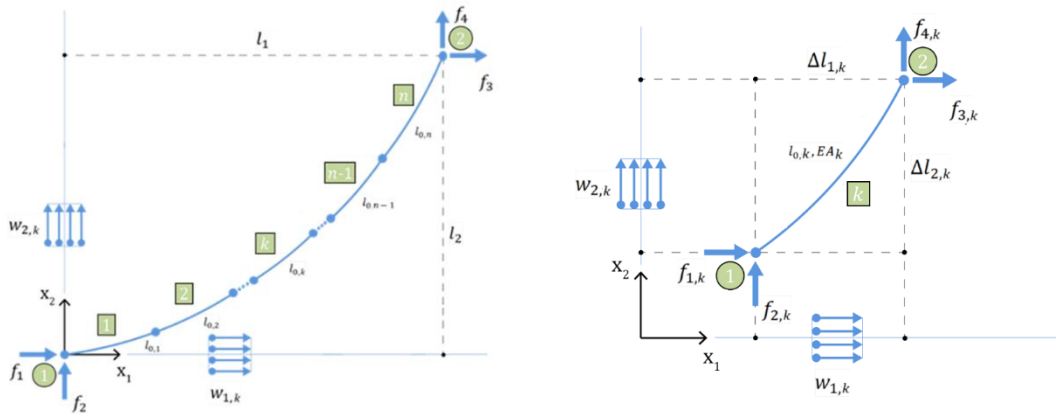


Figure 1. Flowchart of the DynCat formulation.

2.1 Formulation of cable structures under general loads adapted

The mooring line is represented as a sequence of elastic cable elements subjected to horizontal and vertical distributed loads (Abad et al. [7]), as illustrated in Fig. 2a. Each mooring line segment is subdivided in cable elements which are represented as a tension-only structural element, free of bending, shear and torsional stiffness, with constant properties along its length. Figure 2b shows the free-body diagram of a element subjected to generic loadings, with undeformed length $l_{0,k}$ and axial stiffness EA_k.



(a) (b)

Figure 2. Mooring line with "n" elements subjected to generic forces (a) and cable element k (b).

Each element is defined by the coordinates of its end points in the Cartesian x_1 and x_2 directions, with $\Delta l_{1,k}$ and $\Delta l_{2,k}$ variations (also referred as ΔH_k and ΔV_k, respectively). Continuity between elements is ensured by imposing compatibility of the nodal forces. The force at the initial end of element k must be equal the force at the final end of the preceding element $k-1$, such that

$$f_{i,k} = f_{i+2,k-1}, \quad i = 1 \dots 2, \tag{1}$$

and the equilibrium requires that:

$$f_{i+2,k} = -\left(f_{i,k} + w_{i,k} l_{0,k}\right), \quad i = 1 \dots 2. \tag{2}$$

The force components can be generalized to the global mooring-line structure and to the undeformed arc length of any section of element k (s_k), according to the equation

$$f_{i,k}(s_k) = -\left(f_i + \sum_{j=1}^{k-1}\left(w_{i,j} l_{0,j}\right) + w_{i,k} s_k\right), \quad i = 1 \dots 2. \tag{3}$$

Thus, the tensile force magnitude in element k follows:

$$T_k(s_k) = \sqrt{\sum_{i=1}^{2}\left(f_i + \sum_{j=1}^{k-1}\left(w_{i,j} l_{0,j}\right) + w_{i,k} s_k\right)^2}, \quad i = 1 \dots 2. \tag{4}$$

Noting that each element k implies a variation in the positions of its end points in the Cartesian directions, it follows that the variation between the end points of a element is given by

$$\Delta l_{i,k} = -\frac{l_{0,k} f_{i,k}}{EA_k} - \frac{l_{0,k}^2 w_{i,k}}{2EA_k} + \frac{1}{{W_k}^3}\left[W_k w_{i,k}\left(T_{1,k} - T_{2,k}\right) + \left({W_k}^2 f_{i,k} - F_k w_{i,k}\right) ln\left(\frac{\frac{F_k}{W_k} + T_{1,k}}{l_{0,k} W_k + \frac{F_k}{W_k} + T_{2,k}}\right)\right], \tag{5}$$

in which $W_k = \left(\sum_{j=1}^{2} w_{j,k}^2\right)^{1/2}$, $F_k = \sum_{j=1}^{2} f_{j,k} w_{j,k}$, $T_{1,k} = T_k(0)$, $T_{2,k} = T_k\left(l_{0,k}\right)$ and $i = 1 \dots 2$.

Based on the variation of the position of any element k in a Cartesian direction x_i, it follows that these variations compose the predefined projections l_1 and l_2 (H and V, respectively), such that:

$$l_i = \sum_{k=1}^{n} \Delta l_{i,k}\,, \quad i = 1 \dots 2 \tag{6}$$

Equation (6) for indices $i = 1 \dots 2$ has as unknowns the horizontal (f_1) and vertical (f_2) forces in the line applied at the initial end of element $k = 1$, resulting in a nonlinear system of equations solvable by numerical procedure, such as the Newton–Raphson method. Once f_1 and f_2 are determined, the tensile force T_k is defined by eq. (4) and the line geometry follows the equation

$$\begin{aligned} l_{i,k}(s_k) = {} & \frac{1}{{W_k}^3}\left[W_k w_{i,k}\left(T_{1,k} - T_k(s_k)\right) + \left({W_k}^2 f_{i,k} - F_k w_{i,k}\right) \ln\left(\frac{F_k/W_k + T_{1,k}}{s_k W_k + F_k/W_k + T_k(s_k)}\right)\right] - \frac{s_k f_{i,k}}{EA_k} \\ & - \frac{s_k w_{i,k}}{2EA_k} + \sum_{j=1}^{k-1} \Delta l_{i,j}\,, \quad i = 1 \dots 2 \end{aligned} \tag{7}$$

Thus, the necessary parameters are determined and the line is defined and spatially discretized at each time instant t based on the applied loads and geometry corresponding to the fairlead position, whose trajectory $H(t)$ and $V(t)$ is predefined throughout the simulation.

2.2 Kinematic analysis of the line

Once the mooring-line geometry is established for a given time instant, and the prescribed fairlead kinematics — namely its position, velocity, and acceleration components — are known, it becomes possible to determine the velocity and acceleration fields along the mooring line. These fields are essential to account for inertial and hydrodynamic effects in the proposed model.

Considering the horizontal and vertical projections of the line as functions of time, $H(s,t)$ and $V(s,t)$, defined along the undeformed line length s, the local velocities and accelerations in the x and y directions can be obtained by the following equations:

$$\frac{dH}{dt} = \frac{\partial H}{\partial f_x}\frac{df_x}{dt} + \frac{\partial H}{\partial f_y}\frac{df_y}{dt} \tag{8}$$

$$\frac{dV}{dt} = \frac{\partial V}{\partial f_x}\frac{df_x}{dt} + \frac{\partial V}{\partial f_y}\frac{df_y}{dt} \tag{9}$$

$$\frac{d^2H}{dt^2} = \frac{\partial^2 H}{\partial f_x^2}\left(\frac{df_x}{dt}\right)^2 + 2\frac{\partial^2 H}{\partial f_y \partial f_x}\frac{df_x}{dt}\frac{df_y}{dt} + \frac{\partial^2 H}{\partial f_y^2}\left(\frac{df_y}{dt}\right)^2 + \frac{\partial H}{\partial f_x}\frac{d^2 f_x}{dt^2} + \frac{\partial H}{\partial f_y}\frac{d^2 f_y}{dt^2} \tag{10}$$

$$\frac{d^2V}{dt^2} = \frac{\partial^2 v}{\partial f_x^2}\left(\frac{df_x}{dt}\right)^2 + 2\frac{\partial^2 V}{\partial f_y \partial f_x}\frac{df_x}{dt}\frac{df_y}{dt} + \frac{\partial^2 V}{\partial f_y^2}\left(\frac{df_y}{dt}\right)^2 + \frac{\partial V}{\partial f_x}\frac{d^2 f_x}{dt^2} + \frac{\partial V}{\partial f_y}\frac{d^2 f_y}{dt^2} \tag{11}$$

As the line projections result from the adapted cable-element equations — which depend on the tensile components at each end —, their time derivatives, and therefore the rates of change of f_x and f_y, are not directly

accessible. To overcome this limitation, an indirect strategy is adopted: as the fairlead's velocities and accelerations are prescribed, the adapted cable-element equations are differentiated and, by evaluating them at the fairlead, a system of eqs. (8)-(11) is assembled to obtain the time derivatives of the horizontal and vertical tensile forces. Applying these derivatives along the line produces the velocity and acceleration profiles for each section s of the line (Fig. 3), reflecting the structure's instantaneous elastic response to the imposed fairlead kinematics.

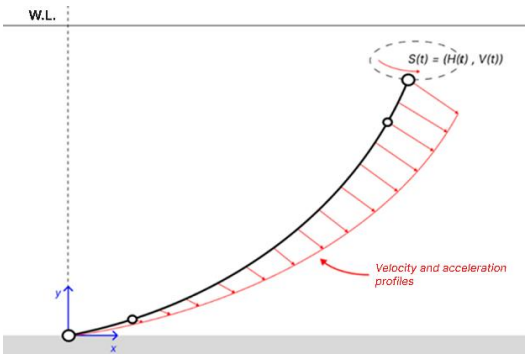


Figure 3. Velocity or acceleration profile along the line, resulting from the fairlead's imposed kinematics.

2.3 Dynamic loads

Fluid–structure interaction forces are obtained using Morison's formulation [8], originally developed to describe the horizontal force on a vertical cylinder fixed to the seabed and extending to the free surface under wave and/or current action. However, Morison's original formulation does not accurately capture mooring-line behavior under dynamic loading, where flow is typically oblique to the curved element axis. To account for this, the Morison force model as presented by Chakrabarti [9] is adopted. Thus, the equation in its most general form is described as:

$$\{df_a\} = \frac{1}{2}\rho C_d^n dA^n v^n |v^n| \{\hat{n}\} + \frac{1}{2}\rho C_d^t dA^t v^t |v^t| \{\hat{t}\} + \rho C_m dV \{\dot{v}\}. \tag{12}$$

Furthermore, the differential inertial force of the cable itself $\{dp\}$ for a discretizing line element dl, is obtained by the equation

$$\{dp\} = -\{a\} A \rho dl. \tag{13}$$

Once the drag and inertial terms from Morison's formulation and the cable's own inertial force at each node are discretized, the horizontal and vertical dynamic loads $w_{1,k}$ and $w_{2,k}$ along each element k from the heterogeneous mooring line can be obtained, respectively, from the following eqs.:

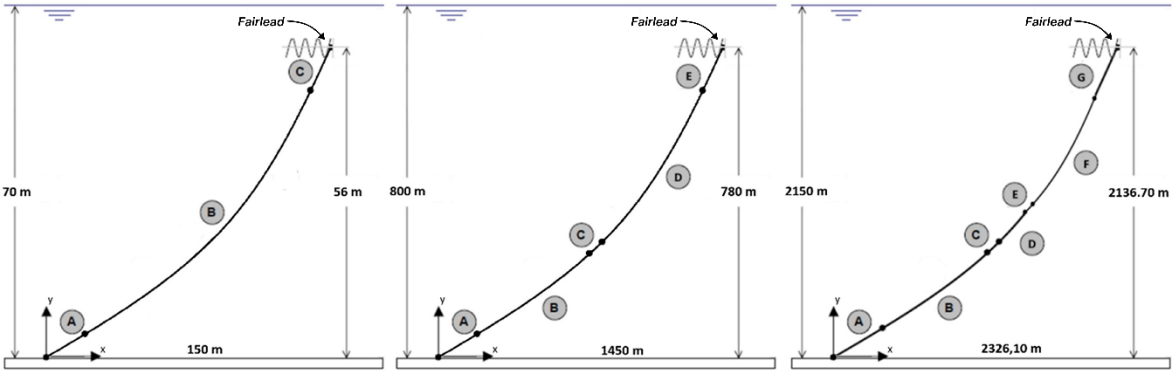
$$w_{1,k} = \frac{\sum F_{x,k}}{l_{0,k}} \geq 0; \tag{14}$$

$$w_{2,k} = \frac{\sum F_{y,k}}{l_{0,k}} - w_{0,k} \leq -0.2\, min(\{w_0\}), \tag{15}$$

in which $\{w_0\}$ is the submerged linear weight vector of each element k. This procedure not only incorporates the dynamic loads into the mathematical model but also mitigates numerical instabilities during the dynamic simulation, which could occur due to an instantaneous geometric inversion of a line element caused by a sudden reversal in load direction or by predominantly horizontal loads causing loss of the catenary shape, as noted by Trubat [10].

3 Results

To evaluate DynCat's performance, case studies were conducted in which its results were compared to those obtained with the reference DOOLINES framework — a widely used tool for nonlinear, static, and dynamic analyses of offshore structures such as risers and mooring lines (Silveira et al. [1]). At this stage of the study, three depth scenarios — shallow, intermediate, and deep — are considered, in the absence of waves and currents, with prescribed fairlead kinematics (scenarios "a", "b" and "c" in Fig. 4, respectively) and with line properties detailed in Tabs. 1, 2 and 3.



(a) (b) (c)

Figure 4. Shallow (a), intermediate (b) and deep (c) water scenarios.

Table 1. Properties of mooring line segments according to material type.

Type	Segment	EA [kN]	Diameter [m]	w_0 [kN/m]	C_d^n	C_d^t	C_m^t	C_m^t
Chain	A, C, E and G	1164903	0.12	2.439	2.4	1.15	2.0	1.0
Polyester	B, D and F	222113	0.225	0.0833	1.6	0.008	2.0	1.0

Table 2. Lengths of line segments in meters.

Scenario	A	B	C	D	E	F	G
a	30.00	120.00	10.00	-	-	-	-
b	150.00	600.00	20.00	600.00	300.00	-	-
c	350.00	839.10	10.00	888.46	10.00	888.46	177.65

Table 3. Number of cable elements by segments.

Scenario	A	B	C	D	E	F	G
a	30	24	10	-	-	-	-
b	15	30	2	30	30	-	-
c	43	83	1	89	1	89	19

In this parametric study, fairlead excitations are independently applied in the x and y directions, in according to the general operability limitation criteria for floating units from NORDFORSK [11], in the form

$$l_i(t) = l_{i,m} + \Delta l \, sin(\omega t), \tag{16}$$

in which l_i represents the projection at time t, $l_{i,m}$ is the mean projection and Δl is the amplitude in the horizontal or vertical direction, while ω is the oscillation frequency defined based on Δl varying from 0 to 10 m horizontally and 0 to 4 m vertically, respecting the kinematic limits presented by NORDFORSK [11]. Figures 5 and 6 show the results of the comparative analysis between DynCat and the reference DOOLINES framework [1] in terms of mean relative error, using time integration steps of Δt of 0.10 s and $0.5\Delta t_{crit}$, respectively.

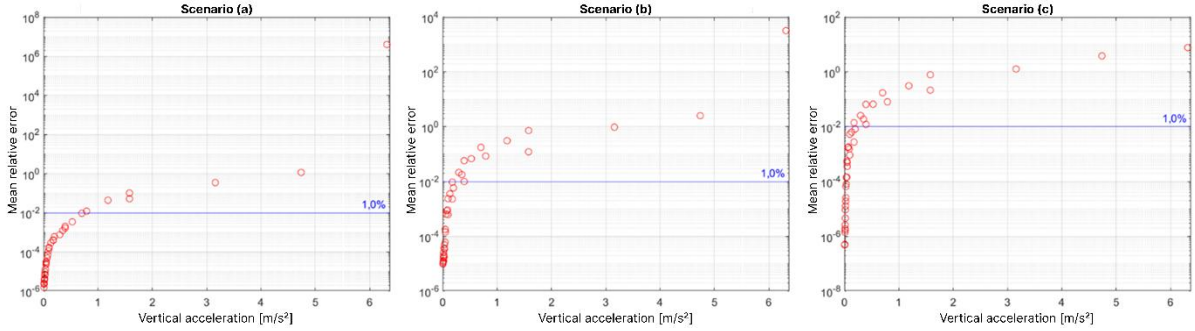


Figure 5. Mean relative errors of the fairlead tensions for the vertical parametric study per scenario.

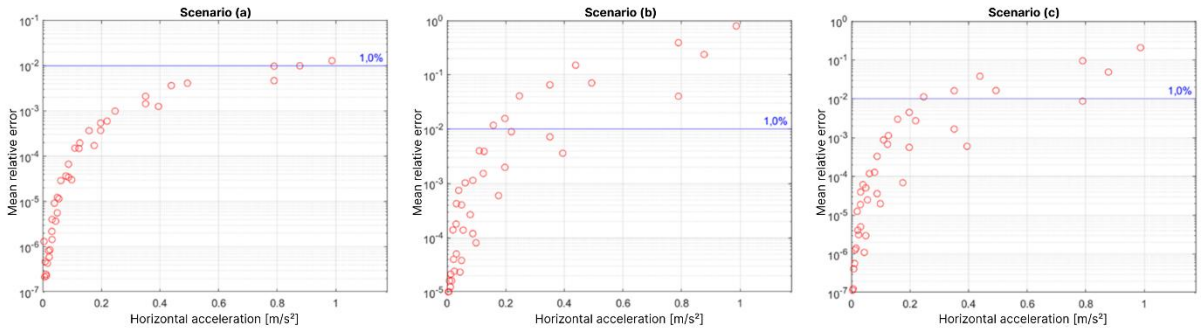


Figure 6. Mean relative errors of the fairlead tensions for the horizontal parametric study per scenario.

DynCat's results show good accuracy in the shallow-water scenario (a), with few cases exceeding mean relative errors of 1% for fairlead accelerations above 1 m/s². However, in the intermediate and deep water scenarios, mean relative errors surpass 1% once the fairlead's horizontal and vertical excitations reach average accelerations above 0.30 m/s².

Next, DynCat is applied to scenario (c) and its results are compared with DOOLINES [1], using horizontal and vertical fairlead excitations shown in Fig. 7, which represent a kinematic behavior of offshore mooring systems, corresponding to maximum accelerations of 0.31 and 0.52 m/s², respectively. The resulting tensile force histories along the line are shown in Fig. 8.

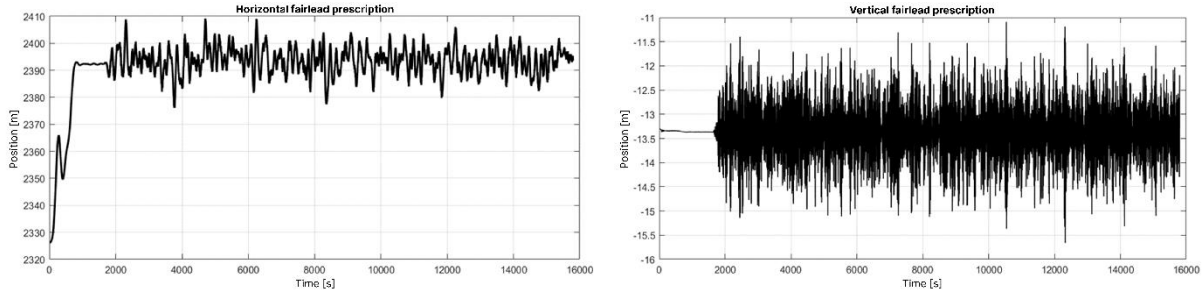


Figure 7. Horizontal (left) and vertical (right) kinematic prescription.

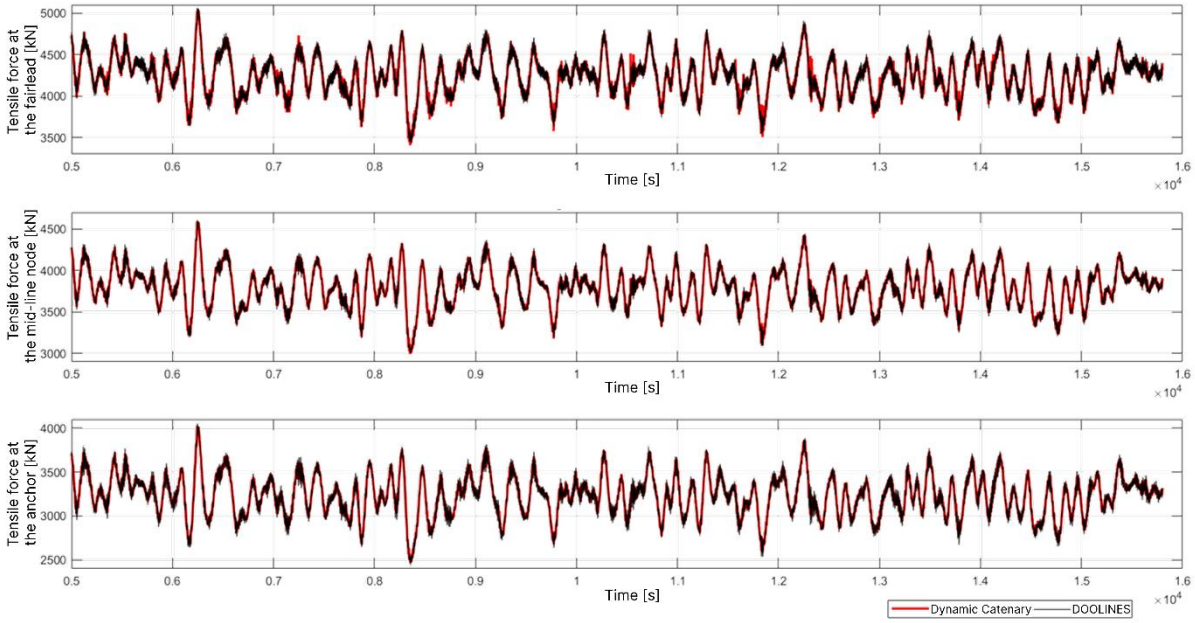


Figure 8. Tensile force histories at the fairlead, at the mid-line node, and at the anchor.

The DynCat formulation shows good agreement with DOOLINES [1], with maximum and mean relative errors of 9.5% and 1.0%, respectively, indicating that the model remains accurate for accelerations up to approximately 0.30 m/s² in deep-water scenarios. Moreover, the DynCat formulation yields a significant reduction in simulation time, ranging from 65.2% to 69.9%.

4 Conclusions

The DynCat methodology was developed based on cable structures under general loadings formulation to efficiently represent the dynamics of mooring lines in a catenary configuration. The results showed good agreement with DOOLINES in shallow water scenarios and limited performance in intermediate and deep waters, while also achieving a significant reduction in computational time — up to 70%. These findings underscore the model's potential as a practical and efficient tool for preliminary mooring-system analyses, offering a favorable balance between accuracy and computational cost. Future work should focus on enhancing the modeling of dynamic loads and considering wave and current loads to improve the model's robustness and applicability under more severe operational conditions.

Acknowledgements. The authors gratefully acknowledge the financial support provided by CNPq and Petrobras.

Authorship statement. The authors hereby confirm that they are the sole liable persons responsible for the authorship of this work, and that all material that has been herein included as part of the present paper is either the property (and authorship) of the authors, or has the permission of the owners to be included here.

References

[1] E. S. S. Silveira, E. N. Lages, and F. M. G. Ferreira, "DOOLINES: An object-oriented framework for non-linear static and dynamic analyses of offshore lines". *Engineering with Computers*, vol. 28, n. 2, pp. 149–159, 2012.
[2] J. Palm, C. Eskilsson and L. Bergdahl, "An hp-adaptive discontinuous Galerkin method for modelling snap loads in mooring cables". *Ocean Engineering*, vol. 144, pp. 266–276, 2017.
[3] M. Hall and A. Goupee, "Validation of a lumped-mass mooring line model with DeepCwind semisubmersible model test data". *Ocean Engineering*, vol. 104, pp. 590–603, 2015.
[4] C. Hao and B. Teng, "Static analysis for a non-uniform flexible mooring cable system". *China Offshore Platform*, vol. 18, n. 4, pp. 18-21, 2003.
[5] T. Fan, D. Qiao and J. Ou, "Optimized Design of Equivalent Truncated Mooring System Based on Similarity of Static and Damping Characteristics". *Twenty-second International Offshore and Polar Engineering Conference*, pp. 959-966, 2012.
[6] P. Trubat, C. Molins, X. Gironella, "Quasi-dynamic mooring line model". *Ocean Engineering*, vol. 243, pp. 110-133, 2022.
[7] M. S. A. Abad, A. Shooshtari, V. Esmaeili and A. N. Riabi. "Nonlinear analysis of cable structures under general loadings". *Finite Elements in Analysis and Design*, vol. 73, pp. 11–19, 2013.
[8] J. R. Morison, M. P. O'Brein, J. W. Johnson and S. A. Schaaf. "The Force Exerted by Surface Waves on Piles". *Journal of Petroleum Technology*, vol. 2, n. 5, pp. 149–154, 1950.
[9] S. K. Chakrabarti. *Handbook of Offshore Engineering* (ed. 1). Elsevier, 2005.
[10] P. Trubat. Station keeping analysis and design for new floating offshore wind turbines. PhD thesis, Universitat Politècnica de Catalunya, Departament d'Enginyeria Civil i Ambiental, 2020.
[11] NORDFORSK, Assessment of Ship Performance in a Seaway: The Nordic Co-operative Project: 'Seakeeping Performance of Ships'. NORDFORSK, 1987.